

Epiphyseal Angulation and Related Spatial Orientation in Slipped Capital Femoral Epiphysis

Theoretical Model and Biomechanical Explanation of Varus and Valgus Slip

Emanuel Gautier, MD, Caroline Passaplan, MD, and Lucienne Gautier, MD

Investigation performed at the Department of Orthopaedic Surgery, HFR–Cantonal Hospital, Fribourg, Switzerland

Background: The management of slipped capital femoral epiphysis (SCFE) is controversial. Surgical decision-making is based regularly on the chronicity, stability, and severity of the slip. The purpose of this study was to determine the true angulation and spatial orientation of the epiphysis in hips with SCFE and contralateral hips.

Methods: Eighteen hips in 18 patients with SCFE were included in the analysis. Trigonometric calculations, based on angle measurements using 2 conventional radiographs in planes that are perpendicular to each other, were used to determine the angulation of the epiphysis and its orientation in space.

Results: The mean absolute epiphyseal obliquity of the SCFE hips was 56.2° and the spatial orientation was 36.5°. The mean obliquity of the contralateral side was 34.0°, with a related spatial orientation of 16.8°. The maximum error can reach up to 9.9° (or 41%) when comparing the calculated angles with the angle measurements on radiographs.

Conclusions: On standard radiographs, the epiphyseal angulation in SCFE is consistently underestimated. As a consequence, the assigned classification of some patients may be 1 severity group too low, which impacts the value of traditional severity classification for surgical decision-making. The analysis of the spatial orientation of the slip with the concomitant direction of the resultant shear can partially explain varus and valgus slip in SCFE.

Level of Evidence: Diagnostic Level IV. See Instructions for Authors for a complete description of levels of evidence.

For patients with slipped capital femoral epiphysis (SCFE), treatment options vary. Surgical procedures include in situ pinning without¹⁻³ or with an open or arthroscopic offset correction^{4,5}, in situ fixation and later intertrochanteric corrective osteotomy^{6,7}, differing techniques of compensatory wedge osteotomy⁸, and the Dunn procedure⁹⁻¹² or modified Dunn procedure¹³⁻²⁶. Performing the modified Dunn procedure with a trochanteric slide approach and surgical hip dislocation facilitates correct reduction of the epiphysis and safe positioning of the hardware in the treatment of SCFE with, for experienced surgeons, lower than historical rates of osteonecrosis of the femoral head²⁷⁻²⁹.

Three classification systems of SCFE are used. The chronological classification³⁰ divides SCFE into the temporally based categories of “chronic,” “acute,” and “acute-on-chronic.” The stability-based classification is related to walking ability and defines SCFE as “unstable” when the patient is unable to walk³¹. The severity-based classification defines SCFE on the

basis of the extent of epiphyseal displacement. A slip angle of <30° is classified as a “minor” slip; 30° to 50°, “moderate”; and >50°, “severe”³². Routine radiographs may underestimate the extent of the displacement and potentially influence the choice of management between in situ pinning and newer methods of anatomic reconstruction with capital realignment³³. Minor slips and post-slip deformity of the proximal part of the femur have a high risk of early damage of the acetabular cartilage and the development of osteoarthritis^{3,34-41}. Thus, the precise analysis of the true slip angle, together with other considerations, is an important factor in surgical decision-making³³. The direction of the slip is only roughly described as a posterior slip or rotation⁴²⁻⁴⁴. We are aware of no previous study in which the angle of epiphyseal obliquity and its precise spatial orientation based on 2 radiographs perpendicular to each other have been calculated. This uncertainty may be a reason why a consensus is missing concerning the best treatment for SCFE⁴⁵.

Disclosure: The authors indicated that no external funding was received for any aspect of this work. The **Disclosure of Potential Conflicts of Interest** forms are provided with the online version of the article (<http://links.lww.com/JBJSOA/A226>).

Copyright © 2020 The Authors. Published by The Journal of Bone and Joint Surgery, Incorporated. All rights reserved. This is an open-access article distributed under the terms of the [Creative Commons Attribution-Non Commercial-No Derivatives License 4.0](https://creativecommons.org/licenses/by-nc-nd/4.0/) (CCBY-NC-ND), where it is permissible to download and share the work provided it is properly cited. The work cannot be changed in any way or used commercially without permission from the journal.

In this study, we aimed to determine the true angles of rotational displacement and the spatial orientation of the epiphysis in hips with SCFE. The spatial position of the epiphysis of the contralateral hips served for comparison. The corresponding trigonometric calculations based on angle measurements on 2 radiographs made in 2 planes perpendicular each other were performed for a series of patients who presented to our department with SCFE.

Materials and Methods

On the anteroposterior view, the epidiaphyseal angle was measured^{32,46,47}. When using the originally described method of the angle measurement³², the epidiaphyseal angle decreases with increasing rotational displacement of the epiphysis in the frontal plane. To avoid this phenomenon, the Southwick supplementary angle corresponding to the epiphyseal inclination was used for the calculations (Fig. 1, left panel). On the lateral view, the angle between a perpendicular to the growth plate and the femoral neck axis was measured (Fig. 1, right panel).

The calculations of the real epiphyseal rotational displacement and the epiphyseal orientation in space were performed as follows (Fig. 2): the measured angle on the anteroposterior radiograph (angle α) is drawn into the X-Z coordinate system, and the angle on the lateral radiograph (angle β), into the Y-Z coordinate system. The adjacents on

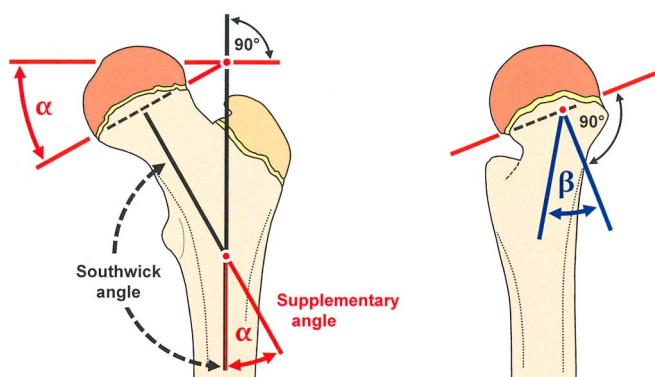


Fig. 1 Illustrations showing the method of measuring epiphyseal obliquity on anteroposterior (left panel) and lateral (right panel) radiographic views. On the anteroposterior radiograph, the medial and lateral end points of the epiphysis are connected by a line. The angle between a line corresponding to the femoral shaft axis and a line perpendicular to the epiphyseal line indicates the obliquity or inclination of the growth plate in the frontal plane. The originally used method of Southwick uses the obtuse angle between these 2 lines, with the disadvantage being that the Southwick angle decreases with increasing epiphyseal obliquity. To overcome this, the acute angle α corresponding to the supplement of the Southwick angle is used for the measurements. On the lateral radiograph, the anterior and posterior end points of the epiphysis are connected by a line. Posterior obliquity is assessed by the angle β between a perpendicular to the epiphyseal line and the femoral neck axis.

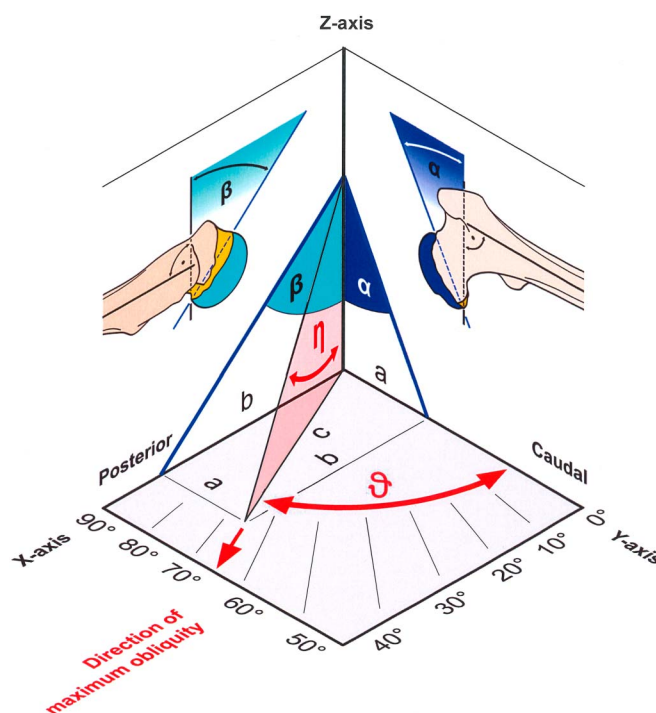


Fig. 2 Assessment of the real epiphyseal obliquity and related spatial orientation. In the frontal and sagittal planes, the diaphysis is oriented parallel to the corresponding X and Y axes. The angles of epiphyseal obliquity on the anteroposterior and lateral views are drawn into the X-Z and Y-Z coordinate systems. The adjacents of the triangles on the Z axis are set to the value 1, corresponding to the radius of the unit circle (for easier calculations). Having measured the epiphyseal obliquity on the anteroposterior radiograph (frontal plane, angle α) and on the lateral view (sagittal plane, angle β), the opposite sides of the triangles a and b are defined as $\tan\alpha$ and $\tan\beta$, respectively. Using the Pythagorean theorem, the hypotenuse c is calculated as the square root of the sum of the squares of a and b. The maximum slip angle η is given by the formula: $\eta = \arctan(c)$. The orientation in space (angle θ) of the maximum slip angle can be calculated by the formula: $\theta = \arctan(b/a)$.

the Z axis are set to the radius of the unit circle (= 1). The opposite side a corresponds to $\tan\alpha$, and the opposite side b, to $\tan\beta$. Using the Pythagorean theorem, the hypotenuse c is calculated as the square root of the sum of the squares of a and b ($c = \sqrt{a^2 + b^2}$). The absolute epiphyseal obliquity (angle η) is given as $\arctan(c)$. The spatial orientation (angle θ) of the epiphyseal obliquity is given as $\arctan(b/a)$ ⁴⁸. Calculations were performed using the absolute angles as measured on the anteroposterior and lateral radiographs for both the hips with SCFE and the contralateral hips and also using the relative angles by subtracting the angles of the contralateral side from the SCFE side in both planes. Appendix 1 provides an Excel (Microsoft) calculation sheet that can be used for assessing the real epiphyseal obliquity, spatial orientation, and the absolute and relative errors between measured and calculated angles. Please be aware that calculations are only possible in the first

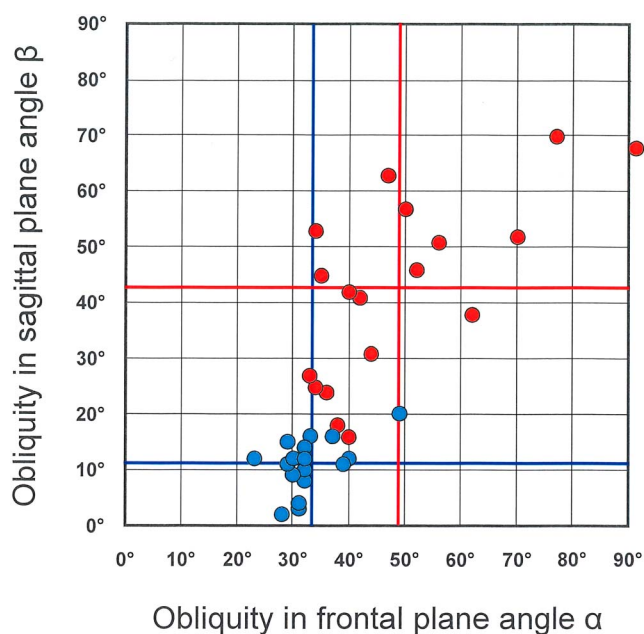


Fig. 3-A

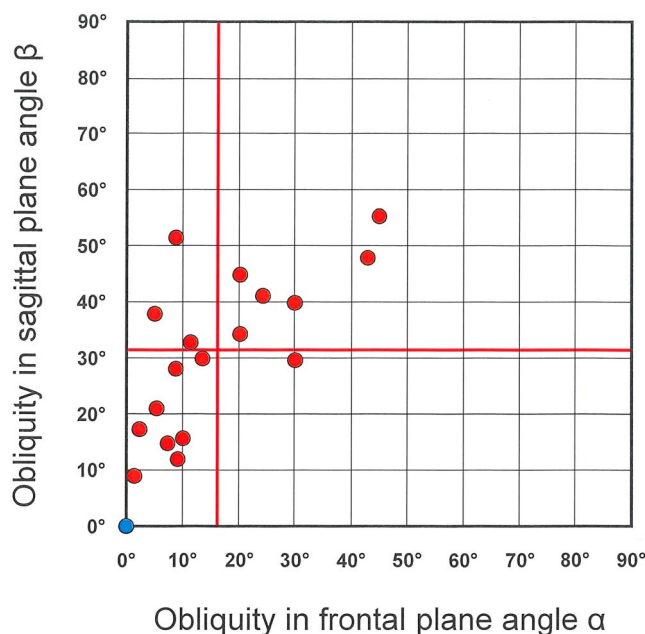


Fig. 3-B

Figs. 3-A and 3-B Absolute and relative angles of epiphyseal obliquity in the frontal and sagittal planes. **Fig. 3-A** Measurements of epiphyseal obliquity of the hips with SCFE (red circles) and contralateral hips (blue circles) in the frontal and sagittal planes. The lines with corresponding colors indicate the mean obliquity measurements in each plane. **Fig. 3-B** The relative slip angles of the hips with SCFE (red circles), after subtraction of the angle of the contralateral hip from that of the SCFE side, are shown. The red lines indicate the mean for each plane. Geometrically, this arithmetic subtraction procedure repositions all contralateral hips to the 0°/0° position of the coordinate system of the figure (blue circle).

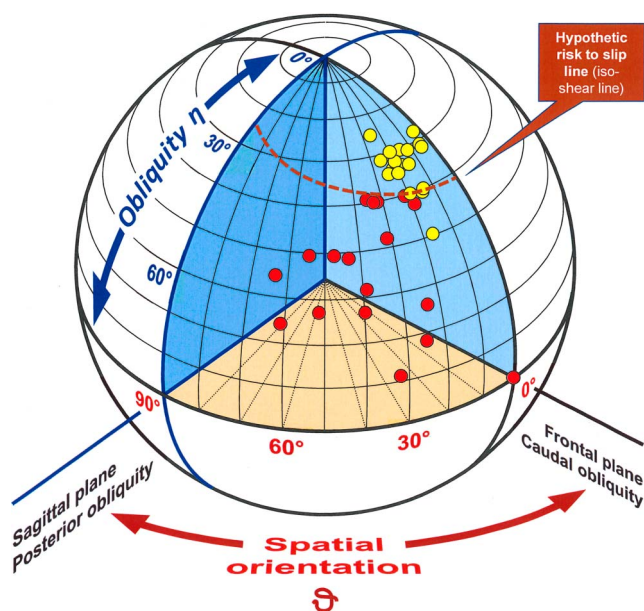


Fig. 4-A

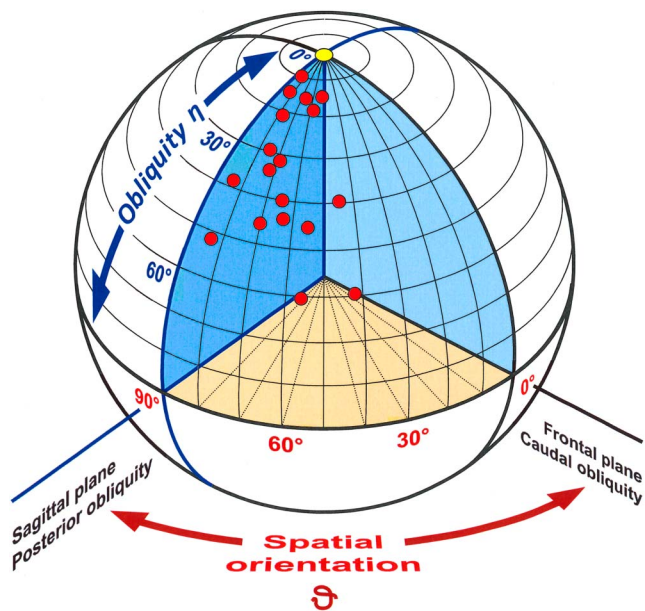


Fig. 4-B

Figs. 4-A and 4-B A 3-dimensional coordinate system allows visualization of the position in space of the epiphyses of the hips with SCFE (red circles) and the contralateral hips (yellow circles). The calculated epiphyseal obliquity (angle η) can be read on the latitude (blue), and its related spatial orientation (angle θ) can be read on the longitude (brown). 0° means an obliquity purely in the frontal plane, and 90°, purely in the sagittal plane. **Fig. 4-A** The absolute epiphyseal position of the SCFE hips and of the contralateral sides. A risk line for epiphyseal slip can be hypothesized, with a critical value of about 25° in the sagittal plane and 45° in the frontal plane. **Fig. 4-B** The relative epiphyseal position after subtraction of the angles of the contralateral side from the SCFE side. Geometrically, such subtraction indicates that all contralateral hips have a 0°/0° position (North Pole position).

TABLE I Radiographic Measurements and Calculated Absolute and Relative Angles*

Parameter	Side	Mean Angle \pm SD ($^{\circ}$)	Range ($^{\circ}$)	95% CI ($^{\circ}$)	P Value (SCFE Vs. Contralateral)
Absolute value					
Frontal angle α	SCFE	49.0 \pm 16.7	33-92	41.3-56.7	<0.001
	Contralateral	32.7 \pm 5.7	23-49	30.1-35.3	
Sagittal angle β	SCFE	42.6 \pm 16.6	16-70	34.9-50.3	<0.001
	Contralateral	11.2 \pm 4.7	2-20	9.0-13.4	
Calculated angle η	SCFE	56.2 \pm 14.5	38.6-89.8	49.5-62.9	<0.001
	Contralateral	34.0 \pm 5.6	25.4-50.3	31.4-36.6	
Spatial orientation θ	SCFE	36.5 \pm 15.9	0.4-63.1	29.2-43.9	<0.001
	Contralateral	16.8 \pm 6.7	3.8-26.6	13.7-19.9	
Relative value: $\Delta_{\text{SCFE} - \text{contralateral}}$					
Frontal slip angle α		16.3 \pm 13.3	1-45	10.2-22.5	
Sagittal slip angle β		31.4 \pm 14.1	9-56	24.9-37.9	
Calculated slip angle η		34.1 \pm 15.2	9.1-60.8	27.1-41.1	
Spatial orientation of slip θ		67.0 \pm 12.5	45-83.9	61.2-72.8	

*SD = standard deviation, and CI = confidence interval.

quadrant from 0° to 90° , where the angles have positive values. Appendix 2 provides instructions for using the Excel sheet.

To illustrate the impact of this theoretical model on the severity classification, the series of patients presenting with SCFE in our department were included in

TABLE II Influence of the Calculated Angles on the Severity Classification

Patient	Absolute Angles ($^{\circ}$)					
	Contralateral Side			SCFE Side		
	Frontal Angle α	Sagittal Angle β	Calculated Angle η	Frontal Angle α	Sagittal Angle β	Calculated Angle η
1	32	14	33.9	77	70	79.0
2	31	4	31.2	40	16	41.6
3	32	12	33.4	52	46	58.7
4	33	16	35.4	34	25	39.4
5	23	12	25.4	35	45	50.7
6	49	20	50.3	92	68	89.8
7	29	15	31.6	34	53	56.1
8	30	9	30.9	33	27	38.6
9	32	8	32.6	62	38	63.8
10	30	12	31.6	50	57	62.8
11	31	3	31.1	36	24	40.4
12	40	12	40.9	70	52	71.7
13	28	2	28.1	38	18	40.2
14	32	10	33.0	56	51	62.6
15	32	14	33.9	40	42	50.9
16	29	11	30.4	42	41	51.4
17	39	11	39.8	47	63	65.9
18	37	16	38.9	44	31	48.7
Total no.						

*SCFE minus contralateral. †Bolded values demonstrate the change in classification, from moderate to severe.

the analysis. The study was approved by the Cantonal Ethics Commission.

The angles as measured on the radiographs were compared with the calculated angles using the previously described mathematical functions. In addition, absolute (in degrees) and relative (in percent) error calculations as a function of the measured angles in the frontal and sagittal planes were performed. All measurements and calculations are based on the assumption that all radiographs were made correctly in 2 planes perpendicular to each other using the technique described by Hafner and Meuli⁴⁹.

Statistical analysis was performed using WinSTAT (R. Fitch Software). The level of significance was set to $p < 0.05$. Normal distribution of all parameters was tested with the Kolmogorov-Smirnov test. Because most parameters were not normally distributed, we only used the nonparametric Mann-Whitney U test for independent variables.

Results

Eighteen patients who had unilateral SCFE were included in the mathematical analysis. The mean age was 12.9 years (range, 6.8 to 17 years). There were 2 female and 16 male patients. In 14 patients, the left hip was involved, and in 4, the

right hip. Fourteen hips were classified as stable, and 4, unstable; 1 slip was acute, 15 were acute-on-chronic, and 2 were chronic.

In the frontal plane, the mean angle of epiphyseal inclination was 49.0° on the side with SCFE and was 32.7° on the contralateral side. In the sagittal plane, the mean angle of posterior epiphyseal angulation was 42.6° and 11.2° for the hips with SCFE and contralateral hips, respectively (Fig. 3-A). According to the originally described method³², slip angles are not defined as absolute but as relative angles, by subtracting the angle of the normal, contralateral side from that of the slipped side. The relative slip was 16.3° in the frontal plane and 31.4° in the sagittal plane (Fig. 3-B). Using the presented trigonometric formula, the calculated real angles were quite different: the absolute epiphyseal obliquity angle (angle η) was, on average, 56.2° for the hips with SCFE and 34.0° for the contralateral hips. The spatial orientation angle (angle θ) of this maximum epiphyseal obliquity was 36.5° and 16.8° for the SCFE and contralateral hips, respectively (Fig. 4-A). Taking the relative angles as the basis for the calculations, the mean relative slip angle (η_{slip}) can reach 34.1° , and the related spatial orientation (θ_{slip}) of the slip can reach 67.0° (Fig. 4-B). See Table I for additional details.

Using the traditional severity score, 7 hips presented with a mild slip; 9, moderate; and 2, severe. After having cal-

TABLE II (continued)

Relative Angles* (°)		Calculated Angle η Using Relative Angles	Severity Classification						Error	
Frontal Angle α	Sagittal Angle β		Traditional Angles†			Calculated Angles†			Absolute Error (°)	Relative Error (%)
			<30°	30-50°	>50°	<30°	30-50°	>50°		
45	56	60.8			56		60.8		4.8	8.6
9	12	14.8	12			14.8			2.8	23.3
20	34	37.5		34			37.5		3.5	10.3
1	9	9.1	9			9.1			0.1	1.1
12	33	34.3		33			34.3		1.3	3.9
43	48	55.4		48			55.4		7.4	15.4
5	38	38.2		38			38.2		0.2	0.5
3	18	18.1	18			18.1			0.1	0.6
30	30	39.2		30			39.2		9.2	30.7
20	45	46.8		45			46.8		1.8	4.0
5	21	21.5	21			21.5			0.5	2.4
30	40	45.5		40			45.5		5.5	13.8
10	16	18.6	16			18.6			2.6	16.3
24	41	44.3		41			44.3		3.3	8.0
8	28	28.8	28			28.8			0.8	2.9
13	30	31.9		30			31.9		1.9	6.3
8	52	52.2			52		52.2		0.2	0.4
7	15	16.4	15			16.4			1.4	9.3
			7	9	2	7	8	3	** Expression is faulty **	

		Epiphyseal obliquity in lateral view angle β																
		5°	10°	15°	20°	25°	30°	35°	40°	45°	50°	55°	60°	65°	70°	75°	80°	85°
Epiphyseal obliquity in antero-posterior view angle α	5°	7.1	11.1	15.7	20.5	25.4	30.3	35.2	40.2	45.1	50.1	55.0	60.0	65.0	70.0	75.0	80.0	85.0
	10°	11.1	14.0	17.8	22.0	26.5	31.1	35.8	40.6	45.4	50.3	55.2	60.1	65.1	70.0	75.0	80.0	85.0
	15°	15.7	17.8	20.8	24.3	28.3	32.5	36.9	41.4	46.0	50.7	55.5	60.3	65.2	70.1	75.0	80.0	85.0
	20°	20.5	22.0	24.3	27.2	30.6	34.3	38.3	42.4	46.8	51.3	55.8	60.5	65.3	70.2	75.1	80.0	85.0
	25°	25.4	26.5	28.3	30.6	33.4	36.6	40.1	43.8	47.8	52.0	56.4	60.9	65.5	70.3	75.1	80.0	85.0
	30°	30.3	31.1	32.5	34.3	36.6	39.2	42.2	45.5	49.1	52.9	57.0	61.3	65.8	70.4	75.2	80.1	85.0
	35°	35.2	35.8	36.9	38.3	40.1	42.2	44.7	47.5	50.7	54.1	57.8	61.8	66.1	70.6	75.2	80.1	85.0
	40°	40.2	40.6	41.4	42.4	43.8	45.5	47.5	49.9	52.5	55.5	58.9	62.5	66.5	70.8	75.3	80.1	85.0
	45°	45.1	45.4	46.0	46.8	47.8	49.1	50.7	52.5	54.7	57.3	60.2	63.4	67.1	71.1	75.5	80.1	85.0
	50°	50.1	50.3	50.7	51.3	52.0	52.9	54.1	55.5	57.3	59.3	61.7	64.6	67.8	71.5	75.7	80.2	85.0
	55°	55.0	55.2	55.5	55.8	56.4	57.0	57.8	58.9	60.2	61.7	63.7	66.0	68.8	72.1	76.0	80.3	85.0
	60°	60.0	60.1	60.3	60.5	60.9	61.3	61.8	62.5	63.4	64.6	66.0	67.8	70.1	72.9	76.3	80.4	85.1
	65°	65.0	65.1	65.2	65.3	65.5	65.8	66.1	66.5	67.1	67.8	68.8	70.1	71.8	74.0	76.9	80.6	85.1
	70°	70.0	70.0	70.1	70.2	70.3	70.4	70.6	70.8	71.1	71.5	72.1	72.9	74.0	75.6	77.8	81.0	85.1
	75°	75.0	75.0	75.0	75.1	75.1	75.2	75.2	75.3	75.5	75.7	76.0	76.3	76.9	77.8	79.3	81.6	85.2
	80°	80.0	80.0	80.0	80.0	80.0	80.1	80.1	80.1	80.1	80.2	80.3	80.4	80.6	81.0	81.6	82.9	85.5
	85°	85.0	85.0	85.0	85.0	85.0	85.0	85.0	85.0	85.0	85.0	85.0	85.1	85.1	85.1	85.2	85.5	86.5

Fig. 5-A

		Epiphyseal obliquity in lateral view angle β																
		5°	10°	15°	20°	25°	30°	35°	40°	45°	50°	55°	60°	65°	70°	75°	80°	85°
Epiphyseal obliquity in antero-posterior view angle α	5°	41.1	11.3	4.9	2.6	1.5	0.9	0.6	0.4	0.2	0.2	0.1	0.1	0.0	0.0	0.0	0.0	0.0
	10°	11.3	40.0	18.5	10.1	6.0	3.7	2.4	1.5	1.0	0.6	0.4	0.2	0.1	0.1	0.0	0.0	0.0
	15°	4.9	18.5	38.3	21.6	13.1	8.3	5.3	3.4	2.2	1.4	0.8	0.5	0.3	0.1	0.0	0.0	0.0
	20°	2.6	10.1	21.6	36.2	22.4	14.4	9.4	6.1	4.0	2.5	1.5	0.9	0.5	0.2	0.1	0.0	0.0
	25°	1.5	6.0	13.1	22.4	33.6	21.9	14.5	9.6	6.3	4.0	2.5	1.4	0.8	0.4	0.1	0.0	0.0
	30°	0.9	3.7	8.3	14.4	21.9	30.8	20.6	13.8	9.1	5.9	3.7	2.2	1.2	0.6	0.2	0.1	0.0
	35°	0.6	2.4	5.3	9.4	14.5	20.6	27.8	18.9	12.6	8.2	5.2	3.1	1.7	0.8	0.3	0.1	0.0
	40°	0.4	1.5	3.4	6.1	9.6	13.8	18.9	24.7	16.8	11.1	7.1	4.2	2.3	1.2	0.5	0.1	0.0
	45°	0.2	1.0	2.2	4.0	6.3	9.1	12.6	16.8	21.6	14.5	9.4	5.7	3.2	1.6	0.7	0.2	0.0
	50°	0.2	0.6	1.4	2.5	4.0	5.9	8.2	11.1	14.5	18.6	12.2	7.6	4.3	2.2	0.9	0.3	0.0
	55°	0.1	0.4	0.8	1.5	2.5	3.7	5.2	7.1	9.4	12.2	15.7	10.0	5.8	3.0	1.3	0.4	0.0
	60°	0.1	0.2	0.5	0.9	1.4	2.2	3.1	4.2	5.7	7.6	10.0	13.0	7.8	4.1	1.8	0.5	0.1
	65°	0.0	0.1	0.3	0.5	0.8	1.2	1.7	2.3	3.2	4.3	5.8	7.8	10.4	5.7	2.6	0.8	0.1
	70°	0.0	0.1	0.1	0.2	0.4	0.6	0.8	1.2	1.6	2.2	3.0	4.1	5.7	8.0	3.8	1.2	0.2
	75°	0.0	0.0	0.0	0.1	0.1	0.2	0.3	0.5	0.7	0.9	1.3	1.8	2.6	3.8	5.7	2.0	0.3
	80°	0.0	0.0	0.0	0.0	0.0	0.1	0.1	0.1	0.2	0.3	0.4	0.5	0.8	1.2	2.0	3.6	0.6
	85°	0.0	0.0	0.0	0.0	0.0	0.0	0.0	0.0	0.0	0.0	0.0	0.1	0.1	0.2	0.3	0.6	1.7

Fig. 5-B

Figs. 5-A and 5-B Error calculations with respect to the measured angles of the epiphyseal obliquity in the frontal and sagittal planes. Yellow to red shadings of the squares indicate an increasingly large error between measured and calculated angles. **Fig. 5-A** Calculated epiphyseal obliquity (in degrees) as a function of the measured angles on the anteroposterior (angle α) and lateral radiographs (angle β). The maximum error is 9.9°, in a case of combined frontal and sagittal plane obliquity of 40° each. **Fig. 5-B** Percentage errors made when angles are not corrected by trigonometric calculations. As an example, an epiphyseal obliquity on the anteroposterior radiograph (angle α) of 30° combined with an obliquity of 25° in the lateral projection (angle β) corresponds in reality to an obliquity (angle η) of 36.6° (blue square, **Fig. 5-A**), and thus to a relative error of 21.9% (blue square, **Fig. 5-B**). This means that a hip with SCFE having slipped distally as well as posteriorly can change the category of the severity of slip classification from mild to moderate, or from moderate to severe.

culated the real relative slip angle, 1 hip in the SCFE group was reclassified, from moderate to severe slip (Table II).

Error calculations taking into account combinations of caudal and posterior obliquity angles showed that the maximum error occurs when the caudal obliquity (angle α) equals the posterior obliquity (angle β). The error reaches up to 9.9°, or 41.1% (Figs. 5-A and 5-B). In our cohort of patients, the absolute slip angles were underestimated, on average, by 2.6° (range, 0.1° to 9.2°) or, on average, 8.8% (range, 0.4% to 30.7%).

Discussion

The aim of our analysis was to assess the real absolute epiphyseal obliquity angles and the relative slip angles and related spatial orientation in hips with SCFE and contralateral hips using 2 radiographs perpendicular to each other. To perform the calculations, the methodology used for the analysis of posttraumatic deformities in long bones was adopted⁴⁸.

Our analysis revealed that the epiphyseal slip angles in SCFE hips and the epiphyseal angulation in the contralateral hips were underestimated compared with the values as measured on standard radiographs. Error calculations showed that that the maximum error can reach up to 10°, or 41.1%.

SCFE can be classified using 3 systems. The chronological classification divides SCFE into the categories of chronic, acute, and acute-on-chronic SCFE³⁰. However, the history of the

patient is difficult to assess because the patient and the parents often do not remember the exact date of the onset of hip symptoms. The stability-based classification is related to the ability to walk³¹. According to Ziebarth et al., epiphyseal stability as reported preoperatively is not correlated with the stability of the epiphysis found during surgery⁵⁰. Thus, this classification is only of relative value for the choice of treatment. The severity-based classification is based on the slip angles as measured on radiographs. Arbitrarily, an angle of <30° is classified as a minor slip; 30° to 50°, as a moderate slip; and >50°, as a severe slip³².

The threshold angle of 30° differentiates only hips presenting with a minor slip from hips with a moderate slip; we are aware of no information in the literature providing a definitive threshold angle for differentiating between a normally positioned hip and a hip with a minor slip. However, this seems to be an important factor for the decision-making concerning prophylactic pinning of the contralateral hip. It is recommended that stabilization of the contralateral hip be performed when, in the lateral view, the absolute angle of posterior tilt exceeds 20°^{51,52}. Thus, this proposal relies only on the lateral radiograph without taking into account the 3-dimensional nature of epiphyseal slipping. We are convinced that, in this context, the spatial orientation of the epiphyseal obliquity is also important. In our series, the mean spatial orientation of the epiphyseal obliquity was 36.5° for the hips with SCFE but

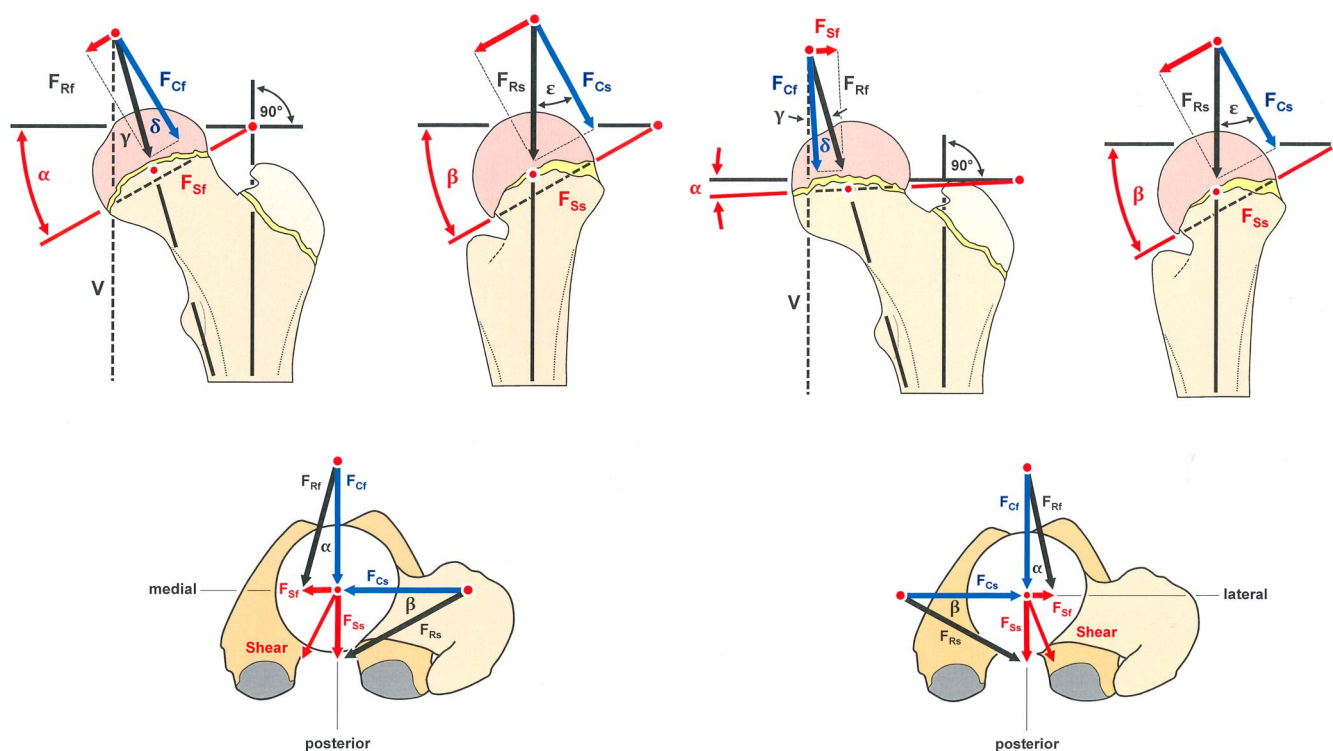


Fig. 6-A

Fig. 6-B

Figs. 6-A and 6-B The amount and direction of the shear force acting on the growth plate. **Fig. 6-A** With increasing obliquity of the growth plate, the shear force on the epiphysis increases and the compressive force decreases. The resultant force acting on the femoral head is divided in its components of shear and compression. In the frontal plane, the resultant force (F_{Rf}), and thus its action line on the hip joint, is 16° divergent (angle γ) with respect to the vertical axis (V)⁷⁵. Angle α is the measured absolute obliquity of the epiphysis, angle δ is the angle between the resultant force and the direction of its compressive-force component (F_{Cf}), and perpendicular to F_{Cf} the amount of shear force acting on the growth plate (F_{Sf}) is visualized—using the method of the parallelogram of forces. In the sagittal plane, the resultant force (F_{Rs}) is parallel to the vertical axis. When the posterior obliquity angle β equals the caudal obliquity angle α , the amount of shear force toward the posterior direction is clearly much higher than in the frontal plane. Angle ϵ , which is defined as the angle between the resultant force (F_{Rs}) and its compressive-force component (F_{Cs}), equals angle β . No divergence of the resultant force in this plane is present, and thus, angle ϵ does not need to be corrected by subtracting 16° . The resultant shear force points with its action line much more toward the posterior direction than the caudal direction, explaining why the epiphysis in SCFE slips mainly toward the posterior direction. **Fig. 6-B** A valgus slip in a case of a hypervalgus hip is illustrated. In the frontal plane, the growth plate is oriented close to 0° , and in the sagittal plane, a posterior slip is present. The resultant vector of the shear force points in the posterolateral direction, which is interpreted in the anteroposterior radiograph as a valgus slip. Depending on the epiphyseal obliquity in space, anteromedial and anterolateral slips can also be imagined. α = the angle of caudal obliquity (inclination) of the growth plate; γ = the angle of divergence of the resultant force of the hip with respect to the vertical axis (16°); δ = the angle between the resultant force and the force component perpendicular to the growth plate ($= \alpha - \gamma$); F_{Rf} = the resultant force on the hip in the frontal plane; F_{Cf} = the compressive-force component in the frontal plane ($= F_{Rf} \cos \delta$); F_{Sf} = the shear-force component in the frontal plane ($= F_{Rf} \sin \delta$); β = the angle of posterior obliquity of the growth plate; ϵ = the angle between the resultant force and the force component perpendicular to the growth plate in the sagittal plane ($= \beta$); F_{Rs} = the resultant force on the hip in the sagittal plane; F_{Cs} = the compressive-force component in the sagittal plane ($= F_{Rs} \cos \epsilon$); and F_{Ss} = the shear-force component in the sagittal plane ($= F_{Rs} \sin \epsilon$).

only 16.8° for the contralateral hips. More longitudinal, long-term outcome studies with a precise definition of the epiphyseal position of the contralateral hip are needed to be able to differentiate between normally positioned hips, “silent slip” hips, and hips with late femoroacetabular impingement due to an undiagnosed or underestimated minor slip.

Our data showed that epiphyseal slip and angulation are underestimated when taking measurements on radiographs. Thus, the severity classification is not precise. When the calculated real angles are taken in consideration, some patients may change from one severity group to the next-higher severity group.

In addition, the severity classification relies on relative angles, because the measured angles of the contralateral side are subtracted from those on the SCFE side for both the anteroposterior and the lateral radiograph. It remains debatable whether these conventionally reported relative slip angles are reliable for a classification system. Subtracting the angles of the contralateral side from those of the affected side indirectly assumes that the contralateral side is completely normal. Given that a high percentage of SCFE cases present with a bilateral pathology⁵³⁻⁶¹ and prophylactic stabilization of the contralateral hip is commonly recommended to avoid progressive deformity

of the contralateral side^{53,55,56,60,62-68}, the contralateral, asymptomatic hip may not then be classified as normal and thus, should not serve as reference to define the severity of the slip. In addition, other long-term studies show a high prevalence of proximal femoral deformity in the contralateral hip in patients treated for unilateral SCFE^{36,55,56,68}. The contralateral asymptomatic hip should be classified as potentially being a pre-slip or silent hip^{69,70}.

To overcome some of the problems with the present classifications, a novel staging system⁷¹ of SCFE was proposed, relying on the so-called epiphyseal tubercle situated on the posterosuperior quadrant of the growth plate and playing the role of the major stabilizer or keystone of the epiphysis⁷². This staging shows a high correlation with the severity of the slip, but moderate and negligible correlation with the stability and chronicity classification, respectively⁷¹. A more recent analysis revealed that hips with SCFE have a smaller epiphyseal tubercle and larger peripheral epiphyseal cupping compared with healthy hips. The authors concluded that a smaller epiphyseal tubercle may be either a predisposing morphologic factor or a consequence of the increased shearing stress across the physis secondary to the slip⁷³.

Biomechanical forces at the hip may cause separation of the growth plate due to shear overload⁷⁴. There is a competition between forces trying to displace the epiphysis and forces trying to stabilize it. The displacing force is the shear force acting parallel to the obliquely oriented plane of the growth plate. The stabilizing force is the compressive force, being perpendicular to the epiphyseal growth plate, creating compression and friction at the interface. In the single-leg standing position, the resultant force acting on the hip joint in the frontal plane is 16° divergent with respect to the vertical axis⁷⁵. The absolute obliquity of the growth plate and the spatial orientation of compression and shear forces are probably the most important mechanical factors causing the epiphyseal slip. In this context, only the shear force and the direction of its action line are of interest. The action line of the shear force on the growth plate points, in most SCFE hips, much more toward the posterior direction than the caudal direction, explaining why epiphyseal slipping is mainly toward the posterior direction (Fig. 6-A). However, with the 3-dimensional vector diagram, the valgus slip in SCFE can be at least partially explained. With a valgus slip, the epiphyseal inclination in the frontal plane is regularly very low⁷⁶⁻⁸⁰, and thus the shear component of the resultant force points toward the posterolateral direction; this is interpreted on an anteroposterior radiograph as a valgus slip (Fig. 6-B).

We are convinced that a measurement system not relying on the contralateral hip but indicating the absolute angle of epiphyseal slip and the absolute angle of the spatial orientation of this maximum slip would be more useful and reliable.

Our data as well as biomechanical reflections suggest that the risk for epiphyseal slipping depends on the absolute amount of epiphyseal obliquity as well as its spatial orientation. Because of the 16° divergence of the resulting force

with respect to the vertical axis, epiphyseal obliquity in the sagittal plane is more susceptible to slipping than in the frontal plane. The critical angle in the sagittal plane must be around 25°, and in the frontal plane, around 45°. Depending on the spatial orientation of the slip, the critical values are situated between 25° and 45°.


Our study had limitations. First, the number of involved patients was relatively small, but they serve only to illustrate the methodology of calculations. Second, all patients with SCFE were included regardless of the chronicity and stability of the slip. Third, correct calculations require a perfect exposure of the femoral neck in 2 planes perpendicular to each other, which may be difficult to obtain for some patients. And fourth, to our knowledge, there are no normative data available regarding the epiphyseal angulation of normal hips to support the hypothesis of a critical angle for the occurrence of a slip.

Strengths of this study include the following: first, trigonometric calculations are precise when based on perfect radiographs made in 2 planes perpendicular to each other. Second, to our knowledge, this is the first time that data showing the exact amount and 3-dimensional direction of the slip and epiphyseal obliquity have been presented. Third, accurate assessment of epiphyseal obliquity of the contralateral hip can help to discriminate between a normally positioned hip and a minor slip of the asymptomatic, contralateral side. And fourth, the presented theoretical model allows assessment of the amount and direction of the shear force acting on the epiphysis, which can at least partially explain the phenomenon of the valgus slip.

Conclusions

Generally, classification systems should inform the appropriate treatment and the prognosis of a distinct pathology as well as allow for scientific comparison of the obtained results. All 3 of the traditionally used classification systems for SCFE have a major drawback: difficulty in assessment (chronological classification), classification that may differ from intraoperative findings (stability classification), or underestimation of the real deformity of the proximal part of the femur (severity classification). Newer surgical techniques allow a complete analysis of hip joint pathology and mechanics under direct visualization. Even minor slips can lead to early damage of the articular cartilage and the adjacent labrum in the weight-bearing area of the joint due to femoroacetabular impingement caused by the slip or post-slip deformity of the proximal part of the femur^{81,82}. Accurate analysis of the contralateral hip is needed to discriminate between a truly healthy hip from a hip presenting with an asymptomatic “silent slip” needing prophylactic stabilization. Even when the morphology of the SCFE hip may not be the only factor for surgical decision-making, a more precise analysis of the deformity caused by the epiphyseal slip seems to be needed^{40,83} to take into account not only the real angle of the epiphyseal obliquity or the relative angle of the slip but also the spatial orientation of the slip.

Appendix

 Supporting material provided by the authors is posted with the online version of this article as data supplements at [jbjs.org](http://links.lww.com/JBJSOA/A227) (<http://links.lww.com/JBJSOA/A227>) (<http://links.lww.com/JBJSOA/A228>). ■

Emanuel Gautier, MD¹
 Caroline Passaplan, MD²
 Lucienne Gautier, MD³

¹Department of Orthopaedic Surgery, HFR–Cantonal Hospital, Fribourg, Switzerland

²Department of Orthopaedic Surgery, Balgrist University Hospital, Zurich, Switzerland

³Emergency Department, Cantonal Hospital, Olten, Switzerland

Email address for E. Gautier: emanuel.gautier@h-fr.ch

ORCID iD for E. Gautier: [0000-0003-2876-7986](https://orcid.org/0000-0003-2876-7986)

ORCID iD for C. Passaplan: [0000-0001-8704-8768](https://orcid.org/0000-0001-8704-8768)

ORCID iD for L. Gautier: [0000-0001-7021-6681](https://orcid.org/0000-0001-7021-6681)

References

- Heyman CH, Herndon CH. Epiphyseodesis for early slipping of the upper femoral epiphysis. *J Bone Joint Surg Am.* 1954 Jun;36(3):539-55.
- Johari AN, Pandey RA. Controversies in management of slipped capital femoral epiphysis. *World J Orthop.* 2016 Feb 18;7(2):78-81.
- Ghijssels S, Touquet J, Himpe N, Simon JP, Corten K, Moens P. Degenerative changes of the hip following *in situ* fixation for slipped capital femoral epiphysis: a minimum 18-year follow-up study. *Hip Int.* 2019 Aug 4;1120700019867248. 2019 Aug 4. [Epub ahead of print].
- Herndon CH, Heyman CH, Bell DM. Treatment of slipped capital femoral epiphysis by epiphyseodesis and osteoplasty of the femoral neck. A report of further experiences. *J Bone Joint Surg Am.* 1963 Jul;45(5):999-1012.
- Leunig M, Horowitz K, Manner H, Ganz R. In situ pinning with arthroscopic osteoplasty for mild SCFE: a preliminary technical report. *Clin Orthop Relat Res.* 2010 Dec;468(12):3160-7.
- Imhäuser G. Die Imhäuser Osteotomie bei floridem Gleitprozess. *Z Orthop Ihre Grenzgeb.* 1965;100:312-20.
- Kramer WG, Craig WA, Noel S. Compensating osteotomy at the base of the femoral neck for slipped capital femoral epiphysis. *J Bone Joint Surg Am.* 1976 Sep;58(6):796-800.
- Hiertonn T. Wedge osteotomy in advanced femoral epiphysiolysis. *Acta Orthop Scand.* 1955;25(1):44-62.
- Dunn DM. The treatment of adolescent slipping of the upper femoral epiphysis. *J Bone Joint Surg Br.* 1964 Nov;46:621-9.
- Broughton NS, Todd RC, Dunn DM, Angel JC. Open reduction of the severely slipped upper femoral epiphysis. *J Bone Joint Surg Br.* 1988 May;70(3):435-9.
- Lefort G, Cottalorda J, Bouche-Pillon MA, Lefebvre F, Daoud S. [Open reduction by the Dunn technique in upper femoral epiphysiolysis. Report of 14 cases]. *Chir Pediatr.* 1990;31(4-5):229-34.
- Fron D, Forgues D, Mayrargue E, Halimi P, Herbaux B. Follow-up study of severe slipped capital femoral epiphysis treated with Dunn's osteotomy. *J Pediatr Orthop.* 2000 May-Jun;20(3):320-5.
- Leunig M, Slongo T, Kleinschmidt M, Ganz R. Subcapital correction osteotomy in slipped capital femoral epiphysis by means of surgical hip dislocation. *Oper Orthop Traumatol.* 2007 Oct;19(4):389-410.
- Leunig M, Slongo T, Ganz R. Subcapital realignment in slipped capital femoral epiphysis: surgical hip dislocation and trimming of the stable trochanter to protect the perfusion of the epiphysis. *Instr Course Lect.* 2008;57:499-507.
- Ziebarth K, Zilkens C, Spencer S, Leunig M, Ganz R, Kim YJ. Capital realignment for moderate and severe SCFE using a modified Dunn procedure. *Clin Orthop Relat Res.* 2009 Mar;467(3):704-16. Epub 2009 Jan 14.
- Slongo T, Kakaty D, Krause F, Ziebarth K. Treatment of slipped capital femoral epiphysis with a modified Dunn procedure. *J Bone Joint Surg Am.* 2010 Dec 15;92(18):2898-908.
- Huber H, Dora C, Ramseier LE, Buck F, Dierauer S. Adolescent slipped capital femoral epiphysis treated by a modified Dunn osteotomy with surgical hip dislocation. *J Bone Joint Surg Br.* 2011 Jun;93(6):833-8.
- Massè A, Aprato A, Grappiolo G, Turchetto L, Campacci A, Ganz R. Surgical hip dislocation for anatomic reorientation of slipped capital femoral epiphysis: preliminary results. *Hip Int.* 2012 Mar-Apr;22(2):137-44.
- Madan SS, Cooper AP, Davies AG, Fernandes JA. The treatment of severe slipped capital femoral epiphysis via the Ganz surgical dislocation and anatomical reduction: a prospective study. *Bone Joint J.* 2013 Mar;95-B(3):424-9.
- Sankar WN, Vanderhave KL, Matheney T, Herrera-Soto JA, Karlen JW. The modified Dunn procedure for unstable slipped capital femoral epiphysis: a multi-center perspective. *J Bone Joint Surg Am.* 2013 Apr 3;95(7):585-91.
- Novais EN, Hill MK, Carry PM, Heare TC, Sink EL. Modified Dunn procedure is superior to in situ pinning for short-term clinical and radiographic improvement in severe stable SCFE. *Clin Orthop Relat Res.* 2015 Jun;473(6):2108-17. Epub 2014 Dec 12.
- Davis RL 2nd, Samora WP 3rd, Persinger F, Klingele KE. Treatment of unstable versus stable slipped capital femoral epiphysis using the modified Dunn procedure. *J Pediatr Orthop.* 2019 Sep;39(8):411-5.
- Leunig M, Manner HM, Turchetto L, Ganz R. Femoral and acetabular realignment in slipped capital femoral epiphysis. *J Child Orthop.* 2017 Apr;11(2):131-7.
- Tannast M, Jost LM, Lerch TD, Schmaranzer F, Ziebarth K, Siebenrock KA. The modified Dunn procedure for slipped capital femoral epiphysis: the Bernese experience. *J Child Orthop.* 2017 Apr;11(2):138-46.
- Ziebarth K, Milosevic M, Lerch TD, Steppacher SD, Slongo T, Siebenrock KA. High survivorship and little osteoarthritis at 10-year followup in SCFE patients treated with a modified Dunn procedure. *Clin Orthop Relat Res.* 2017 Apr;475(4):1212-28.
- Lerch TD, Vuilleumier S, Schmaranzer F, Ziebarth K, Steppacher SD, Tannast M, Siebenrock KA. Patients with severe slipped capital femoral epiphysis treated by the modified Dunn procedure have low rates of avascular necrosis, good outcomes, and little osteoarthritis at long-term follow-up. *Bone Joint J.* 2019 Apr;101-B(4):403-14.
- Gautier E, Ganz K, Krügel N, Gill T, Ganz R. Anatomy of the medial femoral circumflex artery and its surgical implications. *J Bone Joint Surg Br.* 2000 Jul;82(5):679-83.
- Ganz R, Gill TJ, Gautier E, Ganz K, Krügel N, Berlemann U. Surgical dislocation of the adult hip a technique with full access to the femoral head and acetabulum without the risk of avascular necrosis. *J Bone Joint Surg Br.* 2001 Nov;83(8):1119-24.
- Ganz R, Huff TW, Leunig M. Extended retinacular soft-tissue flap for intra-articular hip surgery: surgical technique, indications, and results of application. *Instr Course Lect.* 2009;58:241-55.
- Fahey JJ, O'Brien ET. Acute slipped capital femoral epiphysis: review of the literature and report of ten cases. *J Bone Joint Surg Am.* 1965 Sep;47(6):1105-27.
- Loder RT, Richards BS, Shapiro PS, Reznick LR, Aronson DD. Acute slipped capital femoral epiphysis: the importance of physeal stability. *J Bone Joint Surg Am.* 1993 Aug;75(8):1134-40.
- Southwick WO. Osteotomy through the lesser trochanter for slipped capital femoral epiphysis. *J Bone Joint Surg Am.* 1967 Jul;49(5):807-35.
- Monazzam S, Dwek JR, Hosalkar HS. Multiplanar CT assessment of femoral head displacement in slipped capital femoral epiphysis. *Pediatr Radiol.* 2013 Dec;43(12):1599-605. Epub 2013 Jun 23.
- Goodman DA, Feighan JE, Smith AD, Latimer B, Buly RL, Cooperman DR. Subclinical slipped capital femoral epiphysis. Relationship to osteoarthritis of the hip. *J Bone Joint Surg Am.* 1997 Oct;79(10):1489-97.
- Leunig M, Casillas MM, Hamlet M, Hersche O, Nötzli H, Slongo T, Ganz R. Slipped capital femoral epiphysis: early mechanical damage to the acetabular cartilage by a prominent femoral metaphysis. *Acta Orthop Scand.* 2000 Aug;71(4):370-5.
- Fraitzi CR, Käfer W, Nelitz M, Reichel H. Radiological evidence of femoroacetabular impingement in mild slipped capital femoral epiphysis: a mean follow-up of 14.4 years after pinning in situ. *J Bone Joint Surg Br.* 2007 Dec;89(12):1592-6.
- Tannast M, Goricki D, Beck M, Murphy SB, Siebenrock KA. Hip damage occurs at the zone of femoroacetabular impingement. *Clin Orthop Relat Res.* 2008 Feb;466(2):273-80. Epub 2008 Jan 10.

38. Mamisch TC, Kim YJ, Richolt JA, Millis MB, Kordelle J. Femoral morphology due to impingement influences the range of motion in slipped capital femoral epiphysis. *Clin Orthop Relat Res.* 2009 Mar;467(3):692-8. Epub 2008 Oct 22.
39. Hesper T, Bixby SD, Kim YJ, Yen YM, Bowen G, Miller P, Millis MB, Novais EN. Acetabular retroversion, but not increased acetabular depth or coverage, in slipped capital femoral epiphysis: a matched-cohort study. *J Bone Joint Surg Am.* 2017 Jun 21;99(12):1022-9.
40. Millis MB. SCFE: clinical aspects, diagnosis, and classification. *J Child Orthop.* 2017 Apr;11(2):93-8.
41. Sikora-Klak J, Bomar JD, Paik CN, Wenger DR, Upasani V. Comparison of surgical outcomes between a triplane proximal femoral osteotomy and the modified Dunn procedure for stable, moderate to severe slipped capital femoral epiphysis. *J Pediatr Orthop.* 2019 Aug;39(7):339-46.
42. Billing L, Eklöf O. Slip of the capital femoral epiphysis: revival of a method of assessment. *Pediatr Radiol.* 1984;14(6):413-8.
43. Engelhardt P, Roesler H. [Radiometry of epiphyseolysis capitis femoris. A comparison of conventional roentgen study with axial computerized tomography.] *Z Orthop Ihre Grenzgeb.* 1987 Mar-Apr;125(2):177-82. German.
44. Tayton K. Does the upper femoral epiphysis slip or rotate? *J Bone Joint Surg Br.* 2007 Oct;89(10):1402-6.
45. Aprato A, Conti A, Bertolo F, Massè A. Slipped capital femoral epiphysis: current management strategies. *Orthop Res Rev.* 2019 Mar 29;11:47-54.
46. Southwick WO. Slipped capital femoral epiphysis. *J Bone Joint Surg Am.* 1984 Oct;66(8):1151-2.
47. Jones CE, Cooper AP, Doucette J, Buchan LL, Wilson DR, Mulpuri K, d'Entremont AG. Southwick angle measurements and SCFE slip severity classifications are affected by frog-lateral positioning. *Skeletal Radiol.* 2018 Jan;47(1):79-84. Epub 2017 Aug 24.
48. Mast JW, Jakob RP, Ganz R. Planning and reduction technique in fractures surgery. Springer; 1989.
49. Hafner E, Meuli HC. Radiologic examination in orthopaedics: methods and techniques. Hans Huber; 1975.
50. Ziebarth K, Domayer S, Slongo T, Kim YJ, Ganz R. Clinical stability of slipped capital femoral epiphysis does not correlate with intraoperative stability. *Clin Orthop Relat Res.* 2012 Aug;470(8):2274-9. Epub 2012 Apr 10.
51. Park S, Hsu JE, Rendon N, Wolfruber H, Wells L. The utility of posterior sloping angle in predicting contralateral slipped capital femoral epiphysis. *J Pediatr Orthop.* 2010 Oct-Nov;30(7):683-9.
52. Phillips PM, Phadnis J, Willoughby R, Hunt L. Posterior sloping angle as a predictor of contralateral slip in slipped capital femoral epiphysis. *J Bone Joint Surg Am.* 2013 Jan 16;95(2):146-50.
53. Hägglund G, Hansson LI, Ordeberg G, Sandström S. Bilaterality in slipped upper femoral epiphysis. *J Bone Joint Surg Br.* 1988 Mar;70(2):179-81.
54. Loder RT, Aronson DD, Greenfield ML. The epidemiology of bilateral slipped capital femoral epiphysis. A study of children in Michigan. *J Bone Joint Surg Am.* 1993 Aug;75(8):1141-7.
55. Jerre R, Billing L, Hansson G, Wallin J. The contralateral hip in patients primarily treated for unilateral slipped upper femoral epiphysis. Long-term follow-up of 61 hips. *J Bone Joint Surg Br.* 1994 Jul;76(4):563-7.
56. Hägglund G. The contralateral hip in slipped capital femoral epiphysis. *J Pediatr Orthop B.* 1996 Summer;5(3):158-61.
57. Hurley JM, Betz RR, Loder RT, Davidson RS, Alburger PD, Steel HH. Slipped capital femoral epiphysis. The prevalence of late contralateral slip. *J Bone Joint Surg Am.* 1996 Feb;78(2):226-30.
58. Jerre R, Billing L, Hansson G, Karlsson J, Wallin J. Bilaterality in slipped capital femoral epiphysis: importance of a reliable radiographic method. *J Pediatr Orthop B.* 1996 Spring;5(2):80-4.
59. Stasikelis PJ, Sullivan CM, Phillips WA, Polard JA. Slipped capital femoral epiphysis. Prediction of contralateral involvement. *J Bone Joint Surg Am.* 1996 Aug;78(8):1149-55.
60. Castro FP Jr, Bennett JT, Doulens K. Epidemiological perspective on prophylactic pinning in patients with unilateral slipped capital femoral epiphysis. *J Pediatr Orthop.* 2000 Nov-Dec;20(6):745-8.
61. Aronson DD, Loder RT, Breur GJ, Weinstein SL. Slipped capital femoral epiphysis: current concepts. *J Am Acad Orthop Surg.* 2006 Nov;14(12):666-79.
62. Klein A, Joplin RJ, Reidy JA, Hanelin J. Management of the contralateral hip in slipped capital femoral epiphysis. *J Bone Joint Surg Am.* 1953 Jan;35(1):81-7.
63. Emery RJ, Todd RC, Dunn DM. Prophylactic pinning in slipped upper femoral epiphysis. Prevention of complications. *J Bone Joint Surg Br.* 1990 Mar;72(2):217-9.
64. Carney BT, Weinstein SL, Noble J. Long-term follow-up of slipped capital femoral epiphysis. *J Bone Joint Surg Am.* 1991 Jun;73(5):667-74.
65. Ghanem I, Damsin JP, Carioz H. [Contralateral preventive screwing in proximal femoral epiphyseolysis]. *Rev Chir Orthop Reparat Mot.* 1996;82(2):130-6. French.
66. Schultz WR, Weinstein JN, Weinstein SL, Smith BG. Prophylactic pinning of the contralateral hip in slipped capital femoral epiphysis: evaluation of long-term outcome for the contralateral hip with use of decision analysis. *J Bone Joint Surg Am.* 2002 Aug;84(8):1305-14.
67. Kocher MS, Bishop JA, Hresko MT, Millis MB, Kim YJ, Kasser JR. Prophylactic pinning of the contralateral hip after unilateral slipped capital femoral epiphysis. *J Bone Joint Surg Am.* 2004 Dec;86(12):2658-65.
68. Wensaas A, Gunderson RB, Svenningsen S, Terjesen T. Good long-term outcome of the untreated contralateral hip in unilateral slipped capital femoral epiphysis: forty hips with a mean follow-up of 41 years. *J Child Orthop.* 2014 Oct;8(5):367-73. Epub 2014 Sep 30.
69. Lehmann TG, Engesaeter IO, Laborie LB, Lie SA, Rosendahl K, Engesaeter LB. Radiological findings that may indicate a prior silent slipped capital femoral epiphysis in a cohort of 2072 young adults. *Bone Joint J.* 2013 Apr;95-B(4):452-8.
70. Kohno Y, Nakashima Y, Kitano T, Nakamura T, Takamura K, Akiyama M, Hara D, Yamamoto T, Motomura G, Ohishi M, Hamai S, Yukihide I. Subclinical bilateral involvement of the hip in patients with slipped capital femoral epiphysis: a multi-centre study. *Int Orthop.* 2014 Mar;38(3):477-82. Epub 2013 Oct 11.
71. Maranhão DA, Bixby S, Miller PE, Novais EN. A novel classification system for slipped capital femoral epiphysis based on the radiographic relationship of the epiphyseal tubercle and the metaphyseal socket. *JBJS Open Access.* 2019 Nov 8;4(4):e0033.
72. Liu RW, Armstrong DG, Levine AD, Gilmore A, Thompson GH, Cooperman DR. An anatomic study of the epiphyseal tubercle and its importance in the pathogenesis of slipped capital femoral epiphysis. *J Bone Joint Surg Am.* 2013 Mar 20;95(6):e341-8.
73. Novais EN, Maranhão DA, Vairagade A, Kim YJ, Ktiapour A. Smaller epiphyseal tubercle and larger peripheral cupping in slipped capital femoral epiphysis compared with healthy hips: a 3-dimensional computed tomography study. *J Bone Joint Surg Am.* 2020 Jan 2;102(1):29-36.
74. Salter RB, Harris WR. Injuries involving the epiphyseal plate. *J Bone Joint Surg Am.* 1963;45(3):587-622.
75. Pauwels F. *Gesammelte Abhandlungen zur funktionellen Anatomie des Bewegungsapparates.* Springer; 1965.
76. Skinner SR, Berkheimer GA. Valgus slip of the capital femoral epiphysis. *Clin Orthop Relat Res.* 1978 Sep;135:90-2.
77. Loder RT, O'Donnell PW, Didelot WP, Kayes KJ. Valgus slipped capital femoral epiphysis. *J Pediatr Orthop.* 2006 Sep-Oct;26(5):594-600.
78. Venkatadass K, Shetty AP, Rajasekaran S. Valgus slipped capital femoral epiphysis: report of two cases and a comprehensive review of literature. *J Pediatr Orthop B.* 2011 Sep;20(5):291-4.
79. Koczewski P. Valgus slipped capital femoral epiphysis: subcapital growth plate orientation analysis. *J Pediatr Orthop B.* 2013 Nov;22(6):548-52.
80. Amiraian DE, Sarwar Z, Bireley WR 2nd, Moran E. Valgus slipped capital femoral epiphysis with contralateral pre-slip. *Skeletal Radiol.* 2017 Sep;46(9):1261-5. Epub 2017 Apr 28.
81. Ganz R, Parvizi J, Beck M, Leunig M, Nötzli H, Siebenrock KA. Femoroacetabular impingement: a cause for osteoarthritis of the hip. *Clin Orthop Relat Res.* 2003 Dec;417:112-20.
82. Novais EN, Millis MB. Slipped capital femoral epiphysis: prevalence, pathogenesis, and natural history. *Clin Orthop Relat Res.* 2012 Dec;470(12):3432-8.
83. Milone MT, Bedi A, Poultsides L, Magennis E, Byrd JW, Larson CM, Kelly BT. Novel CT-based three-dimensional software improves the characterization of cam morphology. *Clin Orthop Relat Res.* 2013 Aug;471(8):2484-91.